

RSC Advances



This is an *Accepted Manuscript*, which has been through the Royal Society of Chemistry peer review process and has been accepted for publication.

Accepted Manuscripts are published online shortly after acceptance, before technical editing, formatting and proof reading. Using this free service, authors can make their results available to the community, in citable form, before we publish the edited article. This *Accepted Manuscript* will be replaced by the edited, formatted and paginated article as soon as this is available.

You can find more information about *Accepted Manuscripts* in the [Information for Authors](#).

Please note that technical editing may introduce minor changes to the text and/or graphics, which may alter content. The journal's standard [Terms & Conditions](#) and the [Ethical guidelines](#) still apply. In no event shall the Royal Society of Chemistry be held responsible for any errors or omissions in this *Accepted Manuscript* or any consequences arising from the use of any information it contains.

Excited-State deactivation mechanisms of protonated and neutral phenylalanine: a theoretical study

Reza Omidyan*, Mitra Ataelahi and Gholamhassan Azimi

Department of Chemistry, University of Isfahan, 81746-73441 Isfahan, Iran

Abstract

The potential energy (PE) profiles of neutral and protonated phenylalanine, as one of the simplest aromatic amino acids, at different electronic states have been investigated extensively by RI-RI-MP2 and RI-RI-CC2 methods. The PE profiles have been determined, considering the C_{α} - C_{β} and C_{α} - $C_{(COOH)}$ bond stretching following proton transfer respectively to the aromatic ring and CO group, as well as hydrogen detachment reaction coordinates. The calculated results reveal that low-barrier proton transfer process from ammonia to aromatic chromophore, leading the excited system to the C_{α} - C_{β} bond cleavage, plays the most prominent role in deactivation mechanism of excited $PheH^+$ at the origin of the S_1 - S_0 electronic transition. In contrary, for excited neutral phenylalanine at the band origin of the S_1 - S_0 transition, a large barrier of the S_1 profile along the C_{α} - C_{β} bond-stretching hinders the excited system to approach the dissociative part of PE curve. This barrier, may justify large lifetime of the S_1 excited phenylalanine; (nano second range), while a low barrier, on the S_1 PE profile of protonated species along the PT process, interprets the short range lifetime of protonated species; (in pico-second range).

Keywords: Phenylalanine, Excited States, RI-MP2 and RI-CC2 methods, Relaxation Channels, Photodissociation.

1-Introduction

Molecular building blocks of organic systems readily absorb ultraviolet radiation. These molecules exhibit a large degree of photostability¹, originating from quenching of excited

* Corresponding author, E-mail: r.omidyan@sci.ui.ac.ir, reza.omidyan@u-psud.fr, Fax: (+98) 311 6689732

systems through ultrafast non-radiative relaxation processes. Despite their large UV absorption cross-sections, aromatic amino acids like tryptophan, tyrosine, and phenylalanine, show very small fluorescence quantum yields. This observation deals with the presence of fast radiationless processes, which efficiently quench fluorescence^{2, 3}. The radiationless process was assumed to be the ultrafast internal conversion^{2, 4}. This so-called photostability protects these molecules from undesired photoreactions which are triggered by UV irradiation^{5, 6}.

Spectroscopy of aromatic amino acids in molecular beams either in neutral state⁷⁻¹² or protonated forms¹³⁻¹⁵ has been extensively studied. Particularly, tryptophan is the most heavily studied owing to its large absorption cross section, high fluorescence intensity, and its strong sensitivity to the local protein environment¹⁶⁻¹⁸. Although, tyrosine and phenylalanine have weaker UV absorption than tryptophan, understanding of their spectroscopy and photophysical behavior, is important due to their crucial role in biological systems¹⁹⁻²¹.

On the other hand, fluorescence lifetime and intensity of aromatic amino acids are strongly dependent on the pH values of their environment and drop dramatically at low pH. These results, indicate a predominant nonradiative process, occurring after protonation²². H. Shizuka and co-workers²¹ have shown that the fluorescence intensity of tryptophan markedly increases when it complexes with 18-crown-6. This observation suggests that the ammonium group plays a key role in the internal quenching of tryptophan. It has been stated that internal quenching is due to either the hydrogen transfer from ammonia to the ring or to the C=O group, which produce new conformers^{21, 23}. According to recent experimental and theoretical investigations, it has been well established that the C_α-C_β bond stretching plays a prominent role in photophysics of neutral and protonated aromatic amino acids^{6, 24}. According to the experimental observations²³⁻²⁵, it has been evidenced that ¹ππ* state undergoes a proton-transfer reaction from the amino group to the aromatic chromophore, that provides an efficient and fast pathway for internal conversion in protonated tryptophan and tyrosine, while, a photo-fragmentation process occurring on C_α-C_β bond, has been reported as the most prominent relaxation channel for the case of protonated phenylalanine²⁵. Also, in protonated tryptophan, a barrier-free H atom transfer to the carboxylic-acid oxygen through a small barrier have been predicted²³. In addition, it has been well known that photophysical properties of aromatic amino acids depend strongly on the status of the amino and carboxyl groups; (in neutral and protonated states)²⁶.

The conformation of phenylalanine has been comprehensively studied in a supersonic jet by Martinetz *et al.*⁹. They reported laser induced fluorescence spectrum of the S_1 – S_0 transition of jet-cooled phenylalanine and predicted the existence of multiple conformers using laser saturation technique. Later, detailed investigation on the conformation of phenylalanine by IR–UV double resonance spectroscopy with ion detection and by *ab initio* calculations has been presented by Snoek and co-workers⁸.

Regarding the excited state dynamics, in the case of protonated tryptophan (TrpH^+), the S_1 excited-state lifetime was measured to 380 fs following 266 nm excitation, and calculations of the excited-state dynamics, suggest it could be even shorter^{13, 27}. In contrast to protonated tryptophan, protonated tyrosine (TyrH^+) shows a resolved vibronic spectrum and an excited-state lifetime of 22 picosecond following excitation at 266 nm²⁸. In the case of phenylalanine, a combination of conformer-specific infrared, ultraviolet hole-burning spectroscopy was employed to assign structures to the five conformers^{29, 30}. Lee *et al.*³⁰ have reported that the excited state lifetime of several phenylalanine conformers lie between 20-120 nanosecond, while the excited state lifetime of protonated phenylalanine has been estimated to be in the picosecond range²⁴. Nevertheless, little is known from photophysics and photochemistry of amino acids, particularly, their relaxation dynamics are not well identified so far.

In the present paper we report our theoretical results on deactivation mechanisms of protonated phenylalanine (PheH^+) determined by RI-MP2/RI-CC2 methods as well as its neutral analogue. Thus, after summarizing the computational methods, we present ground- and excited-state optimized structures and excitation energies. We discuss and explain the potential energy curves, determined on the basis of several relaxation pathways of protonated phenylalanine, and compare our results with experimental observations on fragmentation dynamics of protonated phenylalanine, taken from literature. The RI-CC2 is the method of choice because it gives reasonable results for medium size organic molecules, for a moderate computational time^{23, 31-37}.

2- Computational details:

The “*ab initio*” calculations have been carried out with the TURBOMOLE (V 6.3) program suit^{38, 39}, making use of the resolution-of-identity⁴⁰ (RI) approximation for the evaluation of the electron repulsion integrals.

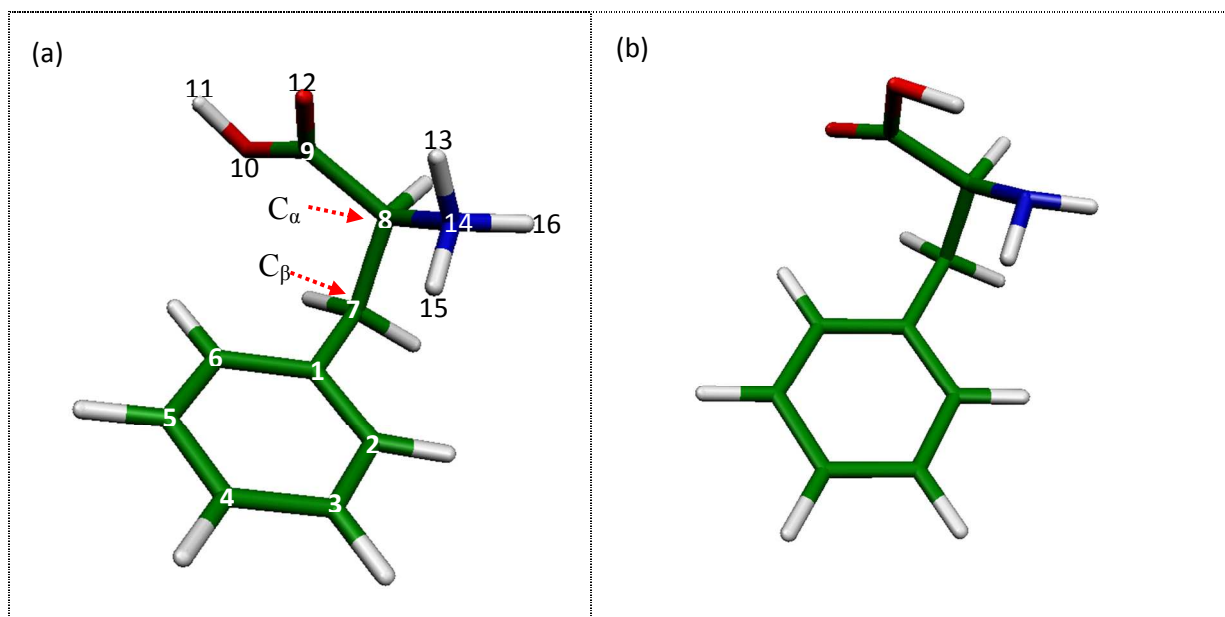


Figure 1: Optimized geometries of (a) Protonated phenylalanine and numbering pattern, (b) the most stable conformer of neutral phenylalanine.

The equilibrium geometry of the titled systems at the ground state has been determined at the RI-MP2 (Möller-Plesset second order perturbation theory) level^{41,42}. Excitation energies and equilibrium geometry of the lowest excited singlet states have been determined at the RI-CC2 (the second-order approximate coupled-cluster method)⁴³⁻⁴⁷.

The dunning's correlation consistent split-valence double- ζ basis set with polarization functions on all atoms (cc-pVDZ)^{48, 49} and the augmented cc-pVDZ by diffuse functions on all atoms (aug-cc-pVDZ)⁵⁰ have been employed. All of potential energy profiles have been determined at the RI-MP2 and RI-CC2 levels, using the aug-cc-pVDZ basis function. The vibrational frequencies in both of the ground and the first excited states were calculated at the MP2 and CC2 levels with the def2-SVP and aug-cc-pVDZ basis sets for neutral and protonated Phenylalanine, respectively in order to confirm the stationary, transition points on the PE profiles and also correcting the adiabatic S_1 - S_0 transition energies with ΔZPE ; (the difference between zero point vibrational energy of ground and S_1 excited states).

The abbreviations of Phe and PheH^+ will be used here after, for neutral and protonated phenylalanine respectively. In order to determine the potential energy profiles, the global

minimum of protonated phenylalanine reported by Rizzo *et al.*¹⁴, has been considered as initial structure of PheH⁺.

In addition, the validity of RI-CC2 method for determination of PE profiles of small organic systems has been established by Aquino and co-workers by comparison with accurate CASPT2 and MR-AQCC data⁵¹. It has been shown that RI-CC2 predicts qualitatively reliable energy profiles of excited state proton transfer reaction. Hence, the RI-CC2 results are trustworthy for qualitative determination of PE profiles⁵²⁻⁵⁹.

3- Results and discussions:

3-A: Ground state equilibrium structures:

The peptide back-bone on the neutral and protonated aromatic amino acids is very flexible, thus, several stable conformers might be available for both forms of neutral and protonated Phe. Nevertheless, it has not been the goal of the present study to perform highly accurate exploration of conformers and geometric structures. We have rather been interested on the development of a clear qualitative picture of the basic mechanisms of nonradiative deactivation processes, especially in the global minimum of protonated phenylalanine, as the simplest aromatic amino acid. Fortunately, comprehensive experimental and theoretical study on conformations of PheH⁺ have been carried out by Stearns and co-workers, where they introduced the global minimum conformer of PheH⁺¹⁴. We have presented this structure in Figure 1-a. As shown, the structure is stabilized by two types of H-bond, the n-terminal hydrogen interacts with the π -system (N-H₁₅... π -ring) of the benzene ring, and another hydrogen atom (H₁₃), nearby the carbonyl oxygen atom, makes the N-H₁₃...O=C hydrogen bonding.

Similar to protonated species, the neutral phenylalanine (Phe), have several stable conformers in the gas phase. The electronic spectrum of phenylalanine in a supersonic jet, employing laser induced fluorescence (LIF) spectroscopy has been recorded by Levy's group⁹. They also identified five different conformers, labeled *A*, *B*, *C*, *D* and *E*, stabilized in the low-temperature environment⁹. Later, Z. Lin *et al.*⁶⁰ by means of the full conformational space exploration, performed a comprehensive theoretical exploration on the phenylalanine, and introduced 37 stable gaseous-conformers for this amino acid molecule.

State	Transition energy/ eV		Oscillator strengths	Configurations
	aug-cc-pVDZ	cc-pVDZ		
Protonated phenylalanine (PheH ⁺)				
S ₁ (¹ ππ*)-Vertical transition energy	5.07	5.17	0.0004	π ₂ π ₁ * (25%), π ₁ π ₂ * (25%), ππ ₁ * (15%)
S ₁ (¹ ππ*)-Adiabatic transition energy [ΔZPE] #ΔE _{exp.}	4.85 [-0.21] #4.65	4.96		
S ₂ (ππ _{CO} *, πσ*)	6.08	6.28	0.0092	π ₃ π _{CO} * (18%), π σ _{NH3} * (14%), σ π _{CO} * (10%)
S ₃ (ππ*)	6.14	6.40	0.0160	π ₂ π ₂ * (28%), π ₁ π ₁ * (22%), π ₂ π ₁ * (21%)
S ₄ (πσ*, ππ*)	6.18	6.90	0.0170	π ₂ σ _{NH3} * (55%), π ₂ π ₂ * (16%), π ₁ σ _{NH3} * (8%)
Neutral phenylalanine (Phe)				
S ₁ (¹ ππ*)-Vertical transition energy	5.08	5.18	0.0005	π ₁ π ₁ * (32%), π ₂ π ₂ * (30%), π ₁ π ₂ * (19%)
S ₁ (¹ ππ*)-Adiabatic Transition energy [ΔZPE] #ΔE _{exp.}	4.84 [-0.20] #4.65	4.99		
S ₂ (nσ*, nπ*)	5.56	5.81	0.0009	n _O σ _{NH3} * (28%), n _O π _{CO} * (20%)
S ₃ (ππ*)	6.04	6.51	0.0204	π ₂ π ₂ * (38%), π ₂ π ₁ * (23%), π ₁ π ₁ * (23%)
S ₄ (nπ*, ππ*)	6.25	7.10	0.0224	n _O π ₁ * (33%), n _O π ₂ * (31%), π ₂ π ₁ * (13%)

Table 1: Excited transition energies, of neutral and protonated phenylalanine, computed at the RI-MP2/RI-CC2 levels with two different basis sets.

The values in brackets represent the difference between zero point vibrational energy of the S₁ excited and ground state in eV.

#The experimental band origin of the S₁-S₀ electronic transition (#ΔE_{exp.}), for protonated and neutral Phenylalanine, have been adopted from Ref. ²⁵ and Ref. ¹⁴ respectively.

It has been well established that the most stable structure of phenylalanine is conformer A (of Levy's group ⁹), corresponding to the optimized structure represented in Figure 1-b. This

structure has been selected in our present work for determination the transition energies and oscillator strength and potential energy profiles of the neutral phenylalanine.

3-B: Excitation energies and molecular orbitals

The calculated vertical transitions energies of neutral and protonated phenylalanine; (most stable conformers), of four lowest singlet transitions (S_1 - S_4), together with adiabatic S_1 - S_0 electronic transition have been tabulated in Table 1. In addition to oscillator strengths, the first four singlet excited-states have been presented. The vertical transition energies respectively for protonated and neutral phenylalanine have been calculated on the optimized geometry of global minimum of protonated and neutral Phenylalanine, shown in Figure 1-a, and 1-b. Within the accuracy of calculation, the vertical S_1 - S_0 transition energy (as well as adiabatic) in protonated and neutral phenylalanine are quite similar, while there is a large discrepancy between the second electronic transition (S_2 - S_0) in neutral and protonated species.

In addition, the optical transition to the lowest excited singlet states (S_1 , S_2) of both neutral and protonated phenylalanine have weak oscillator strength in the UV range. The frontier molecular orbitals (MOs) of protonated and neutral phenylalanine (the most stable conformers) are shown in Table 2. From the RI-RI-CC2 calculations, it is found that the S_1 - S_0 , electronic transition of PheH^+ , gives rise to Homo- \rightarrow Lumo+1 (25%), Homo-1- \rightarrow Lumo+1 (15%) and Homo-1- \rightarrow Lumo+2 (25%) single electron transitions; (Homo and Lumo respectively indicate the highest occupied molecular orbital and the lowest unoccupied molecular orbital). As shown in Table 2, Homo and Homo-1 in PheH^+ are of π nature, and Lumo+1, Lumo+2 are π^* , located on benzene ring. Thus in PheH^+ , the first $^1\pi\pi^*$ is a local transition. According to Table 1 and 2, the S_2 - S_0 transition in Phe and PheH^+ has $n\sigma^*/n\pi^*$ and $\pi\pi^*$ characters respectively.

For neutral phenylalanine, the S_1 state corresponds to the single electron transition from Homo- \rightarrow Lumo (32%), Homo- \rightarrow Lumo+1 (19%) and Homo-1- \rightarrow Lumo+1 (30%);. As shown in Table 2, Homo, and Homo-1 orbitals of Phe are different π orbitals, which are located on the benzene ring. Also, the Lumo, and Lumo+1 are of π^* nature, indicating that the S_1 state of phenylalanine has mostly $\pi\pi^*$ nature.

Protonated phenylalanine (PheH ⁺)							
H-4/ π_3	H-2/ σ_2	H-1/ π_2	H/ π_1	L/ $\sigma_{\text{NH}_3^*}$	L+1/ π_1^*	L+2/ π_2^*	L+3/ π_{CO^*}
Neutral phenylalanine (Phe)							
H-2/ n_o	H-1/ π_1	H/ π_2	L/ π_1^*	L+1/ π_2^*	L+2/ σ_1^*	L+3/ π_{CO^*}	

Table 2: Frontier MOs of protonated and neutral phenylalanine. Only the MOs, having significant contributions to the S_1 - S_4 transitions have been depicted. H and L indicate to Homo and LUMO, respectively.

In order to evaluate our method and basis set, we recalculated the adiabatic S_1 - S_0 electronic transition energies of neutral and protonated Phenylalanine, for which the jet cooled experimental data, is available^{9, 14, 61}; (see Table 2). The S_1 band origin of neutral Phenylalanine has been reported by Martinez *et al.*, amount to $37\,537\text{ cm}^{-1}$ (4.654 eV)⁹ and also for protonated case (PheH⁺), it has been reported to $37\,529\text{ cm}^{-1}$ (4.653 eV) by Stearns¹⁴ and Feraud²⁵. As shown in Table 2, there is good agreement between experimental band origins and our calculated values at the RI-CC2/aug-cc-pVDZ level of theory; ($\Delta E_{(S_1-S_0)}=4.85\text{ eV}$ and 4.84 eV respectively for protonated and neutral species). Nevertheless, considering the difference between zero point vibrational energy of the ground and excited state ($\Delta ZPE=-0.21\text{ eV}$), the S_1 - S_0 transition energy of the RI-CC2/aug-cc-pVDZ level (4.64 eV, ΔZPE corrected), is in the excellent agreement with experimental band origin of PheH⁺, reported by Stearns¹⁴ and Feraud⁶¹ (See Table 1).

3-C. Photophysical behavior: potential energy profiles

3-C-A: Protonated phenylalanine (PheH⁺)

I: C_α - C_β bond stretching (before and after PT to aromatic ring):

The photofragmentation spectrum of protonated phenylalanine (PheH⁺) has been recorded by Stearns *et al.*¹⁴ and most recently by Féraud and co-workers²⁵. One of the most remarkable results of these experiments was observation of specific fragmentation channels. Around the band origin of the S₁-S₀ electronic excitation, the protonated molecule mostly fragments through the C_α-C_β bond rupture^{14,25}, which is the only fragmentation leading to detection of m/z 75 and 92. The former fragment has been assigned to [HOOC-CH₂-NH₂]⁺, and the latter is related to [C₆H₅-CH₂]⁺ and [C₆H₅-CH₃]⁺. We have been motivated to determine the PE profiles relevant to C_α-C_β bond rupture mechanism in two conditions: before and after proton transfer to the benzene ring.

In Figure 2-a, the potential energy profiles calculated along the minimum energy paths (MEP) for bond stretching of the C_α-C_β at the S₀ and S₁ states are shown (full curves, nominated by S₀^(S0) and S₁^(S1)). The coordinate-driven minimum-energy paths have been obtained by fixing the C_α-C_β bond distance and optimizing the lowest S₁ (¹ππ*) state with respect to all other coordinates. The geometry optimizations have been performed with the RI-CC2 method. The energies at the optimized geometries have been calculated at the RI-CC2/aug-cc-pVDZ level.

The PE profiles of the S₀ state, calculated at the ¹ππ*-optimized geometries (dashed lines with hollow circles), as well as at the S₀-optimized geometries, determined with the RI-MP2 method (solid lines with filled circles), are also shown. As shown, the S₁ PE profile along the C_α-C_β bond-stretching coordinate shows a barrier of 0.65 eV. The vibrational frequency analysis at the R_{C_α-C_β}=2.0 Å, shows an imaginary frequency, confirming the transition setae (TS) nature of this point in the middle of reaction coordinate; (See ESI file). Because of the large hindering effect of this barrier, the C_α-C_β bond stretching, before a PT process, is not suggested to play the role of a prominent relaxation-channel for the excited PheH⁺ at the origin of S₀-S₁ transition.

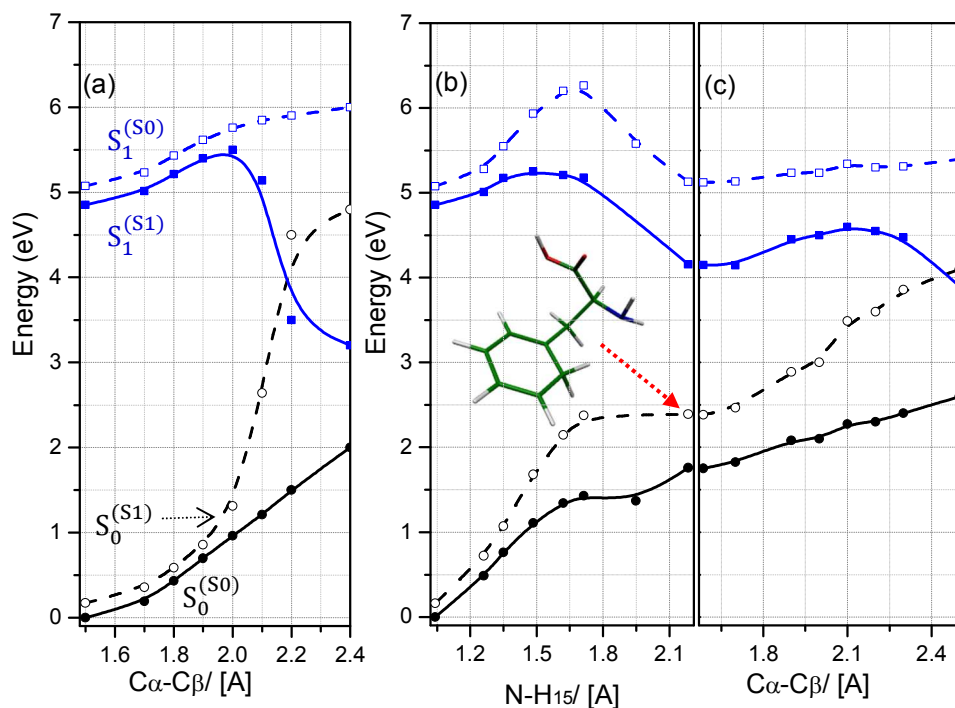


Figure 2. Minimum energy paths (MEPs) of the S_0 state (circles) and the $S_1(\pi\pi^*)$ state (squares), determined at the RI-CC2/aug-cc-pVDZ level as the functions of (a) $C\alpha-C\beta$ bond stretching, (b) $N-H$ bond stretching, (c), $C\alpha-C\beta$ bond stretching after PT in protonated Phenylalanine. The full lines ($S_0^{(S_0)}$ and $S_1^{(S_1)}$) represent the energy profiles of the reaction paths determined in the same electronic state and the dashed lines ($S_0^{(S_1)}$ and $S_1^{(S_0)}$) show the energy profiles determined in the complementary electronic states.

However, according to the seminal work of C. Jouvét and co-workers²³, it has been shown that proton transfer from the ammonium to the benzene ring, is an important deactivation pathway in protonated tryptophan and tyrosine. Thus, we have investigated the minimum energy path (MEP) for PT from ammonia to the cycle in PheH^+ (Figure 2-b). The coordinate-driven minimum-energy paths for PT have been obtained by fixing the proton-transfer coordinates ($N-H_{15}$), containing the $N-H_{15}\dots\pi$ hydrogen bond, and optimizing the lowest $S_1(1\pi\pi^*)$ state geometry with respect to all other coordinates. As shown, the MEP exhibits a transition state at $R_{N-H_{15}}=1.5 \text{ \AA}$, corresponding to the top of the barrier in the middle of reaction coordinate of PT process; ($\Delta E=0.35 \text{ eV}$). Nevertheless, the barrier is not so large and can be overcome by a wave packet prepared at the origin of S_1-S_0 transition. In addition, the tunneling-effect of hydrogen atom through the barrier, since of its slight mass, can be another possibility for passing the barrier and

approaching the excited system to dissociate region of PE profile. In this condition, the excited system may evolve to the C_α - C_β bond rupture.

In Figure 2-c, the MEP for C_α - C_β bond breaking, following the PT process to aromatic ring, has been depicted. As shown, there is a small barrier in the panel c, which is less pronounced than that of its previous panel. This barrier locates roughly under the S_1 band origin of global PheH^+ . Indeed, the C_α - C_β bond cleavage after PT process in such condition can be triggered by proton transfer from ammonia to the benzene ring. Moreover, from inspection of Figure 2-c, it is seen that a conical intersection appears at the end of the reaction coordinate (C_α - $C_\beta \sim 2.5 \text{ \AA}$), where the C_α - C_β bond is almost broken. In such long lengths of C_α - C_β bond, there is no sufficient force to turn the excited system back to the ground state, thus photodissociation of the excited system after the CI, must be more favored.

Additionally, the vibrational frequency analyzing has been carried out for selected points of Figure 2 (a-c). The results have been presented in ESI file. All of the vibrational frequencies for the first points of panel a, and b (Figure 2-a, and 2-b) are positive, confirming the stationary nature of these points on the PE surface. Nevertheless, in Figure 2 a-c, there are three transition states, corresponding to the maximum points of each panel, having one imaginary frequency along the reaction coordinate.

II: PT to C=O and hydrogen detachment reactions:

According to experimental results, by increasing the excitation photon energy, roughly above the band origin of S_1 - S_0 transition, a new fragmentation channel at m/z 120 has been appeared. This fragmentation result has been assigned by Féraud *et al.*²⁵ to the bond breaking of C_8 - C_9 following a proton transfer to the carbonyl group, leading to the formation of iminium ion, CO and H_2O from PheH^+ . This fragmentation channel, has been assigned to C_α - $C_{(\text{COOH})}$ bond breaking, following the PT process from $-\text{NH}_3$ to carbonyl. Indeed, the carbonyl $\text{C}=\text{O}$ group, in addition to $-\text{NH}_2$ and benzene ring, is another electron rich center that attracts proton. When the excess proton locates on the oxygen atom of the carbonyl group ($\text{C}=\text{O}$), it gives an isomer with internal energy of $\sim 0.80 \text{ eV}$ (77.2 kJmol^{-1}) higher than that of global minimum. Nevertheless, we have determined the PE profiles of PT reaction from $-\text{NH}_3$ to $\text{C}=\text{O}$ at the S_1 and S_0 states (Figure 3), in order to obtain more information on PT process at the excited state. The PE profiles of Figure 3- a, have been calculated along the N-H_{13} bond, containing the ($\text{C}=\text{O} \dots \text{H}_{13}$ -N)

hydrogen bond, while in Figure 3- b, the C₈-C₉ bond has been selected as reaction coordinate. Considering the MEP curves in Figure 3-a, in the S₁(ππ*) state, there is a large barrier hindering the excited system to proceed along the reaction coordinate. From Figure 3-a and b, it is seen that a wave packet prepared by excitation of PheH⁺ at the origin of S₁ transition, cannot simply overcome the barriers and proceed to the dissociative region of Figure 3-a and 3-b. Thus, sufficient excess energy more than the band origin of S₁ state of PheH⁺, will be required for opening this dissociation channel.

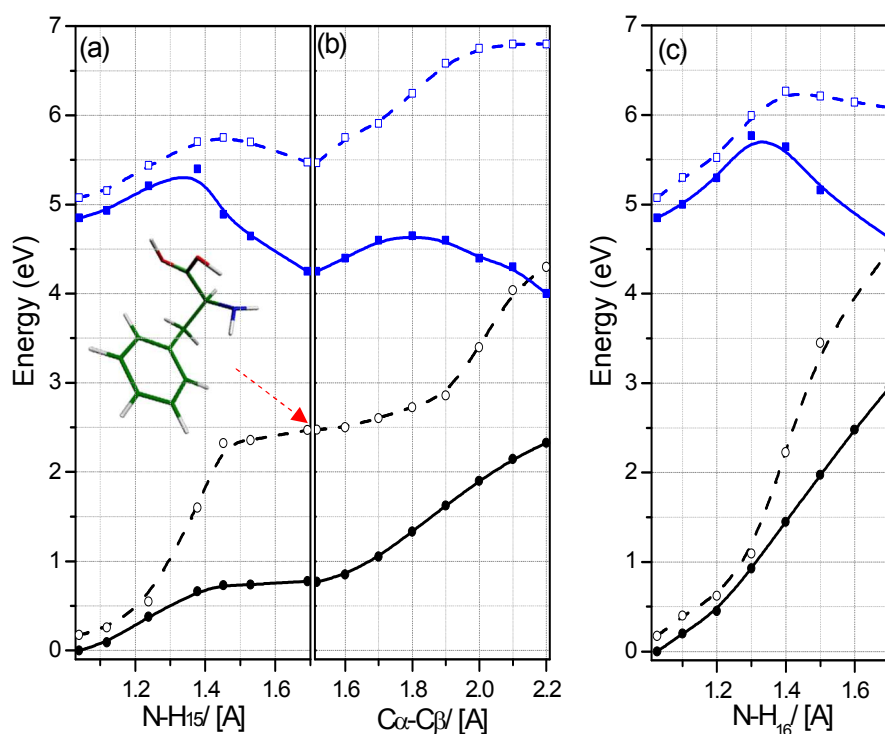


Figure 3. Minimum energy paths (MEPs) of the S₀ state (circles) and the S₁(ππ*) state (squares), determined at the RI-CC2/aug-cc-pVDZ level as a functions of (a) N-H₁₅, and (b) The C_α-C_β bond stretching and (c) the N-H₁₆ in the protonated phenylalanine.

In such condition, the excited system overcomes both barriers of Figure 3 (a and b), and proceeds to the end of reaction coordinate, which is corresponding to the bond cleavage of C_α-C_(COOH). This bond cleavage can be responsible for photo-fragmentation of PheH⁺, producing CO+H₂O fragments, above the band origin of the S₁-S₀ transition.

It is noteworthy that photo-fragment of m/z 120, corresponding to CO+H₂O fragments, has been observed 531 cm⁻¹ (0.065 eV) above the band origin of PheH⁺ by Fraude *et al.*²⁵. However, the RI-CC2, being a single reference method, is unable to precisely determine the crucial points such as conical intersections and potential barriers, and its results are only qualitatively reliable⁵²⁻⁵⁹. Additionally, the CO+H₂O fragments, have been observed in the CID (Collision- Induces Dissociation) experiments too⁶². Thus, there is another possibility that decreasing the S₁, S₀ energy gap of PheH⁺ after proton transfer from ammonia to C=O (Figure 3, panel a), leads the excited system to the ground state via ultrafast internal conversions, then the PheH⁺ system undergoes fragmentation from S₀ PE profile.

The PE profiles, for hydrogen detachment channel has been investigated, as another suggestion for deactivation of PheH⁺. The potential energy profiles calculated along the minimum energy paths (MEP) for N-H₁₆ bond stretching at the S₀ and S₁ states are presented in Figure 3-c. As shown, there is a large barrier in the middle of S₁ PE profile along the reaction coordinate. From Figure 3-c, it is seen that a large barrier of 0.90 eV height, hinders the excited system of the S₁(¹ππ*) state to proceed along the reaction coordinate. Thus the hydrogen detachment deactivation pathway has been predicted to be very unlikely. However, this deactivation mechanism can be opened only when the excited system contains plenty of excess energy; (0.9 eV more than the band origin of S₁-S₀ transition).

Furthermore, the vibrational frequency analysis, verifies the TS nature of the maximum points; (R_{N-H}=1.4 Å and R_{C_α-C_β}=1.8 Å respectively in Figure 3-a and 3-b). However, the calculated vibrational frequencies for the maximum point of the S₁ PE profile of Figure 3-c; (R_{N-H₁₆}=1.4 Å), show more than one imaginary frequencies, indicating to a hilltop nature for this point. The excited system on the hilltop is extremely unstable and may undergo several reactions, among them the N-H stretching lead the excited system to the end of reaction coordinate, where the S₁/S₀ PE profiles, cross with each other and produce a conical intersection in the multi dimensional picture. This CI can be responsible for non radiative deactivation of system, via ultrafast internal conversions.

3-C-B: Neutral Phenylalanine:

Although, UV absorption and fluorescence spectra of phenylalanine and its derivatives have been studied by Wiczek's group⁶³, to our knowledge, there is no extensive theoretical report

on relaxation dynamics and deactivation pathways of this molecule. Nevertheless, long lifetime of the S_1 excited phenylalanine (nanosecond range), reported by Lee *et al.*³⁰, indicates to a stable S_1 character of isolated Phe. Thus, we have determined the PE profiles of phenylalanine, along C_α - C_β bond stretching to obtain more information from photophysics of this system.

In Figure 4, the S_0 , S_1 PE curves along with the C_α - C_β bond stretching have been presented. From inspection of these results, it is seen, that the MEP profile of the S_1 ($\pi\pi^*$) excited state has a rising pattern, showing a TS (e.i a barrier of ~ 0.61 eV magnitude) at the $R_{(C_\alpha-C_\beta)} = 2.0$ Å (see ESI file), then slowly shows a dissociative trend to the end of reaction coordinate. This is while the S_0 PE curve, has a rising trend, and near the end of reaction coordinate ($R=2.3$ Å), the S_1 ($\pi\pi^*$) crosses with the S_0 electronic state, which develops into the conical intersections (CIs) in a multidimensional picture. Nevertheless, only the wave packets prepared in the $^1\pi\pi^*$ state by optical excitation of adequate excess energy (≈ 0.60 eV), is able to pass the barrier and reach to the CI, which is expected to lead the excited system with an internal conversion to the ground state. Thus, the conical intersection of S_1 - S_0 states, at the end of reaction coordinate may mostly play the role of photostabilizer to protect neutral phenylalanine against UV radiation of $\lambda_{\text{ex}} < 240$ nm, via ultrafast internal conversion. Alternatively, from CI region, the excited system may undergo dissociation along the C_α - C_β bond, producing photoproduct radicals.

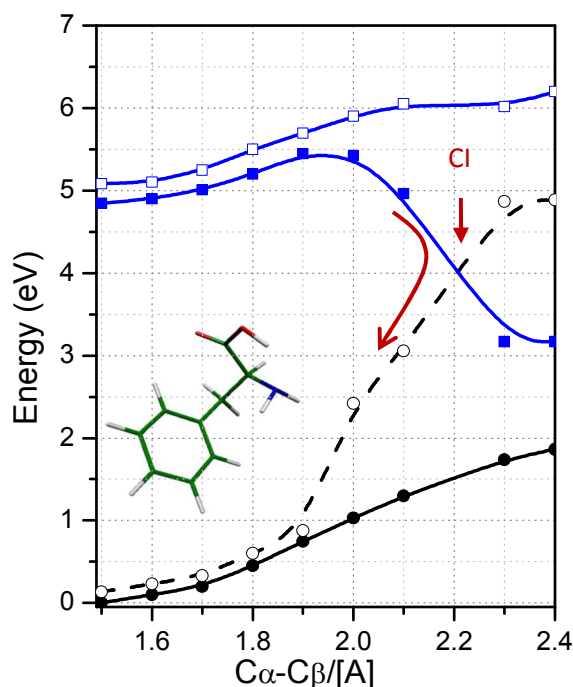


Figure 4: RI-CC2 PE profiles of the electronic ground state (circles) and the lowest excited state (squares) as a function of the C_{α} - C_{β} stretching coordinate in the neutral phenylalanine.

4- Conclusion

Ab initio electronic-structure and reaction-path calculations, at the RI-CC2 level of theory, have been carried out, to characterize the relaxation dynamics in protonated and neutral phenylalanine. The excited state intramolecular proton transfer to the aromatic ring has been predicted to be the most favorable consequence of excitation of PheH^+ at the origin of S_1 - S_0 transition. The low barrier PT process to aromatic chromophore, consequently lead the excited system to the C_{α} - C_{β} bond cleavage. In contrary, the PT process from ammonia to carbonyl group ($\text{C}=\text{O}$), as the same as hydrogen detachment reaction coordinate, involve large hindering barriers along the S_1 potential energy curves. When the excited system contains small excess energy above the band origin of S_1 transition, the excited state PT process to $\text{C}=\text{O}$, leads the excited system to C_{α} - $C_{(\text{COOH})}$ bond breaking. Although, relaxation of PheH^+ along hydrogen detachment pathway should be extremely unlikely at the band origin of S_1 transition, it can be responsible for relaxation of photoexcited system with ~ 0.9 eV excess energy above the band origin.

For neutral phenylalanine, the large lifetime of the S₁ state (nano second) can be justified by lacking nonradiative relaxation channels from origin of S₁ transition to the ground state. The C_α-C_β bond stretching, investigated in this study has a barrier of 0.61 eV magnitude, restricting the excited system to approach the dissociative region and conical intersection. Definitely, this relaxation channel in the neutral phenylalanine can be proposed as the UV protection of phenylalanine, exciting by $\lambda_{\text{ex}} < 240$ nm.

Acknowledgment

The research council of *Isfahan University* is acknowledged for financial support. The authors are greatly indebted to *Prof. C. Jouvét* (University of Aix-Marseille) for helpful comments. The use of computing facility cluster *GMPCS of the LUMAT* federation (FR LUMAT2764) is kindly appreciated.

References:

1. D. Creed, *Photochem. Photobiol.*, 1984, **39**, 537-562.
2. C. E. Crespo-Hernandez, B. Cohen, P. M. Hare and B. Kohler, *Chem. Rev.*, 2004, **104**, 1977-2019.
3. M. B. Robin, *Higher Excited States of Polyatomic Molecules*, Academic, New York, 1972.
4. A. Reuther, H. Iglev, R. Laenen and A. Laubereau, *Chem. Phys. Lett.*, 2000, **325**, 360-368.
5. W. Domcke and A. L. Sobolewski, *Nat. Chem.*, 2013, **5**, 257-258.
6. C.-M. Tseng, M.-F. Lin, Y. L. Yang, Y. C. Ho, C.-K. Ni and J.-L. Chang, *Phys. Chem. Chem. Phys.*, 2010, **12**, 4989-4995.
7. R. Cohen, B. Brauer, E. Nir, L. Grace and M. S. de Vries, *J. Phys. Chem. A*, 2000, **104**, 6351-6355.
8. L. C. Snoek, E. G. Robertson, R. T. Kroemer and J. P. Simons, *Chem. Phys. Lett.*, 2000, **321**, 49-56.
9. S. J. Martinez, J. C. Alfano and D. H. Levy, *J. Mol. Spectrosc.*, 1992, **156**, 421-430.
10. J. M. Bakker, L. M. Aleese, G. Meijer and G. von Helden, *Phys. Rev. Lett.*, 2003, **91**.
11. T. R. Rizzo, Y. D. Park, L. A. Peteanu and D. H. Levy, *J. Chem. Phys.*, 1986, **84**, 2534-2541.
12. L. C. Snoek, R. T. Kroemer, M. R. Hockridge and J. P. Simons, *Phys. Chem. Chem. Phys.*, 2001, **3**, 1819-1826.
13. O. V. Boyarkin, S. R. Mercier, A. Kamariotis and T. R. Rizzo, *J. Am. Chem. Soc.*, 2006, **128**, 2816-2817.
14. J. A. Stearns, S. Mercier, C. Seaiby, M. Guidi, O. V. Boyarkin and T. R. Rizzo, *J. Am. Chem. Soc.*, 2007, **129**, 11814-11820.
15. F. O. Talbot, T. Tabarin, R. Antoine, M. Broyer and P. Dugourd, *J. Chem. Phys.*, 2005, **122**.
16. R. H. Callender, R. B. Dyer, R. Gilmanishin and W. H. Woodruff, *Annu. Rev. Phys. Chem.*, 1998, **49**, 173-202.
17. M. Gruebele, *Annu. Rev. Phys. Chem.*, 1999, **50**, 485-516.

18. T. Q. Liu, P. R. Callis, B. H. Hesp, M. de Groot, W. J. Buma and J. Broos, *J. Am. Chem. Soc.*, 2005, **127**, 4104-4113.
19. C. S. Hoaglund-Hyzer, A. E. Counterman and D. E. Clemmer, *Chem. Rev.*, 1999, **99**, 3037-3079.
20. M. F. Jarrold, *Annu. Rev. Phys. Chem.*, 2000, **51**, 179-207.
21. H. Shizuka, M. Serizawa, T. Shimo, I. Saito and T. Matsuura, *J. Am. Chem. Soc.*, 1988, **110**, 1930-1934.
22. J. R. Lakowicz, *Principles of Fluorescence Spectroscopy*, 2nd ed. edn., Kluwer, Academic/Plenum, New York, 1999.
23. G. Gregoire, C. Jouvét, C. Dedonder and A. L. Sobolewski, *J. Am. Chem. Soc.*, 2007, **129**, 6223-6231.
24. C. Dedonder, G. Féraud and C. Jouvét, in *Photophysics of Ionic Biochromophores*, ed. S. Brøndsted Nielsen, Wyer, Jean Ann, Springer Berlin Heidelberg, Editon edn., 2013, pp. 155-180.
25. G. Féraud, M. Broquier, C. Dedonder, C. Jouvét, G. Grégoire and S. Soorkia, *J. Phys. Chem. A*, 2014, in press, DOI:10.1021/jp5065837

26. J. M. Beechem and L. Brand, *Annu. Rev. Biochem.*, 1985, **54**, 43-71.
27. H. Kang, C. Dedonder-Lardeux, C. Jouvét, S. Martrenchard, G. Gregoire, C. Desfrancois, J. P. Schermann, M. Barat and J. A. Fayeton, *Phys. Chem. Chem. Phys.*, 2004, **6**, 2628-2632.
28. H. Kang, C. Jouvét, C. Dedonder-Lardeux, S. Martrenchard, G. Gregoire, C. Desfrancois, J. P. Schermann, M. Barat and J. A. Fayeton, *Phys. Chem. Chem. Phys.*, 2005, **7**, 394-398.
29. T. Hashimoto, Y. Takasu, Y. Yamada and T. Ebata, *Chem. Phys. Lett.*, 2006, **421**, 227-231.
30. Y. H. Lee, J. W. Jung, B. Kim, P. Butz, L. C. Snoek, R. T. Kroemer and J. P. Simons, *J. Phys. Chem. A*, 2004, **108**, 69-73.
31. I. Alata, R. Omidyan, C. Dedonder-Lardeux, M. Broquier and C. Jouvét, *Phys. Chem. Chem. Phys.*, 2009, **11**, 11479-11486.
32. I. Alata, R. Omidyan, M. Broquier, C. Dedonder, O. Dopfer and C. Jouvét, *Phys. Chem. Chem. Phys.*, 2010, **12**, 14456-14458.
33. M. Schreiber, M. R. Silva-Junior, S. P. Sauer and W. Thiel, *J. Chem. Phys.*, 2008, **128**, 134110.
34. I. Georgieva, N. Trendafilova, A. J. Aquino and H. Lischka, *J. Phys. Chem. A* 2007, **111**, 127-135.
35. B. Chmura, M. F. Rode, A. L. Sobolewski, L. Lapinski and M. J. Nowak, *J. Phys. Chem. A*, 2008, **112**, 13655-13661.
36. B. Saed and R. Omidyan, *J. Phys. Chem. A*, 2013, **117**, 2499-2507.
37. B. Saed and R. Omidyan, *J. Chem. Phys.*, 2014, **140**, 024315.
38. TURBOMOLE, V6.3 2011, a development of University of Karlsruhe and Forschungszentrum Karlsruhe GmbH, 1989-2007, TURBOMOLE GmbH, since 2007; available from <http://www.turbomole.com>.

39. R. Ahlrichs, M. Bär, M. Häser, H. Horn and C. Kölmel, *Chem. Phys. Lett.*, 1989, **162**, 165-169.
40. R. Ahlrichs, *Phys. Chem. Chem. Phys.*, 2004, **6**, 5119-5121.
41. F. Haase and R. Ahlrichs, *J. Comput. Chem.*, 1993, **14**, 907-912.
42. K. Eichkorn, F. Weigend, O. Treutler and R. Ahlrichs, *Theor. Chem. Acc.*, 1997, **97**, 119-124.
43. C. Hättig, *J. Chem. Phys.*, 2003, **118**, 7751-7761.
44. C. Hättig and K. Hald, *Phys. Chem. Chem. Phys.*, 2002, **4**, 2111-2118.
45. C. Hättig and A. Köhn, *J. Chem. Phys.*, 2002, **117**, 6939-6951.
46. C. Hättig and F. Weigend, *J. Chem. Phys.*, 2000, **113**, 5154-5161.
47. A. Köhn and C. Hättig, *J. Chem. Phys.*, 2003, **119**, 5021-5036.
48. T. H. Dunning, *J. Chem. Phys.*, 1989, **90**, 1007-1023.

49. A. Hellweg, C. Hättig, S. Höfener and W. Klopper, *Theor. Chem. Acc.*, 2007, **117**, 587-597.
50. R. A. Kendall, T. H. Dunning and R. J. Harrison, *J. Chem. Phys.*, 1992, **96**, 6796-6806.
51. A. J. A. Aquino, H. Lischka and C. Hättig, *J. Phys. Chem. A*, 2005, **109**, 3201-3208.
52. A. L. Sobolewski and W. Domcke, *Phys. Chem. Chem. Phys.*, 2006, **8**, 3410-3417.
53. A. L. Sobolewski and W. Domcke, *ChemPhysChem*, 2007, **8**, 756-762.
54. A. L. Sobolewski, W. Domcke and C. Hättig, *J. Phys. Chem. A*, 2006, **110**, 6301-6306.
55. J. Jankowska, M. F. Rode, J. Sadlej and A. L. Sobolewski, *ChemPhysChem*, 2012, **13**, 4287-4294.
56. J. Jankowska, M. F. Rode, J. Sadlej and A. L. Sobolewski, *ChemPhysChem*, 2014, **15**, 1643-1652.
57. M. F. Rode, A. L. Sobolewski, C. Dedonder, C. Jouvet and O. Dopfer, *J. Phys. Chem. A*, 2009, **113**, 5865-5873.
58. A. L. Sobolewski and W. G. Domcke, *J. Phys. Chem. A*, 2007, **111**, 11725-11735.
59. A. L. Sobolewski, D. Shemesh and W. Domcke, *J. Phys. Chem. A*, 2008, **113**, 542-550.
60. Z. Huang, W. Yu and Z. Lin, *J. Mol. Struct-THEOCHEM* 2006, **758**, 195-202.
61. G. Feraud, M. Broquier, C. Dedonder-Lardeux, G. Gregoire, S. Soorkia and C. Jouvet, *Phys. Chem. Chem. Phys.*, 2014, **16**, 5250-5259.
62. A. Svendsen, U. J. Lorenz, O. V. Boyarkin and T. R. Rizzo, *Rev. Sci. Instrum.*, 2010, **81**, 073107.
63. A. Rzeska, K. Stachowiak, J. Malicka, L. Lankiewicz and W. Wiczak, *J. Photoch. Photobio. A*, 2000, **133**, 33-38.